Agricultural and Forest Meteorology 281 (2020) 107847

Contents lists available at ScienceDirect

Agricultural and Forest Meteorology

journal homepage: www.elsevier.com/locate/agrformet

Improving estimation of evapotranspiration during soil freeze-thaw cycles by incorporating a freezing stress index and a coupled heat and water transfer model into the FAO Penman-Monteith model

Qiang Xu[a,1], Xiaofei Yan[b,1], David A. Grantz[c], Xuzhang Xue[d], Yurui Sun[a], Peter Schulze Lammers[e], Zhongyi Wang[a], Qiang Cheng[a,*]

[a] College of Information and Electrical Engineering, China Agricultural University, 100083 Beijing, China
[b] School of Technology, Beijing Forestry University, Beijing 100083, China
[c] Department of Botany & Plant Sciences, University of California at Riverside, Kearney Agricultural Center, Parlier, CA, 93648, United States
[d] National Engineering Research Center for Information Technology in Agriculture, 100097 Beijing, China
[e] Department of Agricultural Engineering, The University of Bonn, 53115 Bonn, Germany

ARTICLE INFO

Keywords:
Evapotranspiration
Freeze-thaw cycles
Soil water potential
Model combination
Parameter optimization

ABSTRACT

Evapotranspiration (ET) plays an important role in water and energy balance at the surface-atmosphere interface. It is widely reported that near-surface soil water content (SWC) or soil water potential (SWP) significantly affects ET and this parameter has been incorporated into the FAO Penman-Monteith (FAO-PM) model for prediction of ET during crop growth seasons. However, there is little information on the effect of SWC or SWP on prediction of ET during soil freeze-thaw cycles in winter. We present an experiment conducted at a demonstration farm with a crop of winter wheat, over two winters near Beijing, China. A lysimeter system equipped with a weather station was used to measure the ET flux and meteorological data. Unfrozen soil water content (USWC) and soil temperature (T_{soil}) were measured using dielectric tube sensors (DTS) and digital temperature sensors, respectively. SWP was determined by measured USWC and a soil moisture characteristic (SMC) curve derived from the soil freezing characteristic (SFC) curve and the Clapeyron equation in frozen soil. Detailed measurements in year 1 showed that the FAO-PM model exhibited a complex error pattern, underestimating ET from unfrozen soil but overestimating ET from stable frozen soil. To address these errors, we define a freezing stress index (K_{sf}) as a function of SWP. Incorporation of K_{sf} as a modifier of the standard crop coefficient in the FAO-PM model improved prediction of ET (RMSE declined from 0.424 to 0.187 mm day^{-1}, in year 1). These data revealed a correlation between SWP near the soil surface (< 10 cm) and measured ET over freezing and thawing cycles. We incorporated a coupled heat and water transfer (CHWT) model into the improved FAO-PM model to predict USWC, SWP and ET throughout the winter of year 2 from current meteorological data as upper boundary conditions, initial measurements of ET, USWC and T_{soil} as initial conditions, and K_{sf} and soil hydraulic properties optimized in year 1. The results showed that ET estimation was significantly improved, with RMSE reduced from 0.323 to 0.281 mm day^{-1} using the combined (FAOPM-K_{sf}-CHWT) model. Model error primarily derived from an underestimation of simulated SWP during soil freezing process. The combined model extends the utility of the FAO-PM model to non-cropping seasons including winter in temperate climates and reduces the data requirements for accurate prediction of ET from intermittently frozen soil.

1. Introduction

Evapotranspiration (ET), as outgoing vapor flux at the boundary between soil-plant and atmosphere, is a key variable for water balance, heat exchange, irrigation scheduling, hydrological studies and drought monitoring (Cai et al., 2007; Huo et al., 2012; Sentelhas et al., 2010; Tomas-Burguera et al., 2017). ET can be measured using weighing lysimeters, eddy correlation, bowen ratio and surface renewal techniques (Ali et al., 2018; Haymann et al., 2019; Huo et al., 2012; Rana et al., 2000). These instrumental methods have high measurement accuracy,

* Corresponding author.
E-mail address: chengqiang@cau.edu.cn (Q. Cheng).
[1] These authors contributed equally to this work

https://doi.org/10.1016/j.agrformet.2019.107847
Received 10 May 2019; Received in revised form 16 October 2019; Accepted 14 November 2019
Available online 21 November 2019

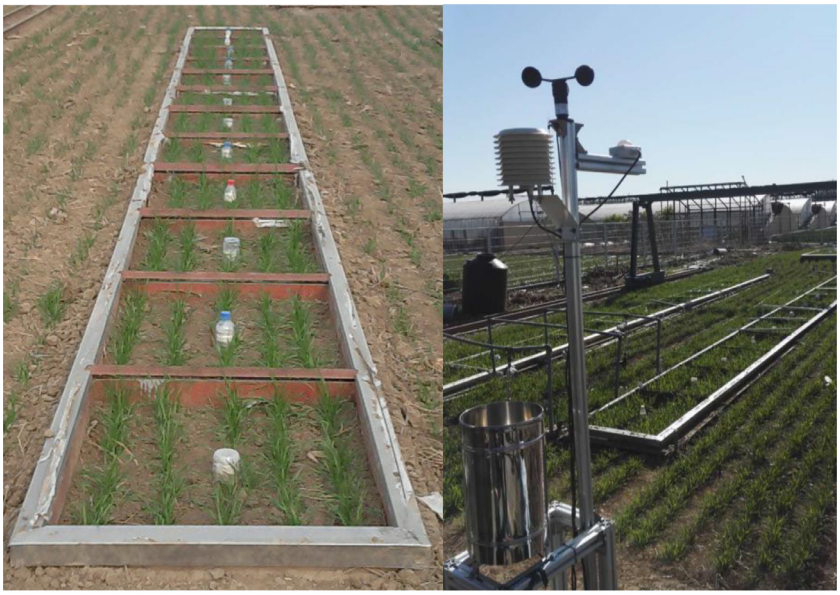

(a) (b)

Fig. 1. Photos of (a) the lysimeter measurement system and (b) the experimental site with weather station at the end of October.

Table 1
Soil parameters at the experimental site.

Parameters	Sand	Silt	Clay	θ_s	K_s
Values	39.9%	46.6%	13.5%	0.41 $m^3\ m^{-3}$	0.02 m h^{-1}

but remain prohibitively expensive for widespread application in many areas of the world (Ali et al., 2018; Huo et al., 2012; Liu et al., 2017). Model-based ET prediction using meteorological data is therefore widely used to estimate ET for crops and other vegetated surfaces (Adebayo et al.,2012; Allen et al., 1998; Ding et al., 2013; Huo et al., 2012; Torres et al., 2011). Among these model-based estimation methods, the FAO Penman-Monteith (FAO-PM) approach with crop-specific coefficients relating ET to reference evapotranspiration (ET_0) has been applied to many different cropping systems.

ET is often highly correlated with near-surface (< 10 cm) soil water content (SWC) or soil water potential (SWP) when reduced soil moisture limits ET to below ET_0 (Bodner et al., 2007; Chanzy et al., 1993; Hssaine et al., 2018; Jiang et al., 2016; Liu et al., 2005; Merlin et al., 2018; Mitchell et al., 2009; Poulovassilis et al., 2001; Raz-Yaseef et al., 2010; Snyder et al., 2000; Zhang et al., 2011; Zhang et al., 2019; Zhao et al., 2018). SWC or SWP has been used to estimate ET using FAO-PM during crop growth (Allen et al., 1998; Phogat et al., 2016; Poulovassilis et al., 2001; Zhao et al., 2018), but has not generally been applied during the off-season, including in winter when freeze-thaw cycles may perturb soil water availability.

Due to the low temperature in winter, the crop coefficients used in FAO-PM approach in the growing season require adjustment during soil freeze-thaw cycles. Allen et al., 1998 and Kang et al. (2003) suggested divergent values of average crop coefficients (K_c = 0.4 and 0.61, respectively), for winter wheat in the winter, but did not explicitly consider the effect of the unfrozen component of available water nor the freeze-thaw status of the underlying soil on the accuracy of the ET estimation.

The main objectives of this study are (i) to explore whether there is an effect of SWP near the frozen soil surface on actual ET and to develop a combined model to reduce data requirements for predicting ET, (ii) to improve the prediction accuracy of the FAO-PM model of ET during soil freeze-thaw cycles using a parameter optimization approach, and (iii) to assess the prediction accuracy of ET estimated by the combined model by comparison with independent measurements in a second winter.

2. Material and methods

2.1. Description of the evapotranspiration (ET) model

ET is a combination of evaporation (E_s) from the soil surface and transpiration (T_r) from the crop canopy. ET is governed by energy exchange at the boundary between soil-plant and atmosphere and is limited by the amount of energy available (Allen et al., 1998; Snyder et al., 2000). Penman (1948) combined the surface energy balance with mass transfer to develop an equation to predict evaporation from saturated bare soil or freely transpiring short grass, as a function of evaporation from open water. In order to characterize plant transpiration under varied species and environmental conditions, Monteith (1965) added a bulk surface resistance term to the Penman equation, yielding the Penman-Monteith (PM) equation, as

$$\lambda ET = \frac{\Delta(R_n - G) + \rho_a c_p\left(\frac{e_s - e_a}{r_a}\right)}{\Delta + \gamma\left(1 + \frac{r_s}{r_a}\right)} \quad (1)$$

where ET is evapotranspiration flux (mm day^{-1}); R_n is net radiation (MJ m^{-2} day^{-1}); G is soil heat flux density (MJ m^{-2} day^{-1}); λ is the latent heat of vaporization (MJ kg^{-1}), Δ is the slope of the vapor pressure curve (kPa $^{\circ}C^{-1}$); γ is the psychrometric constant (kPa $^{\circ}C^{-1}$); e_s is saturation vapor pressure (kPa); e_a is actual vapor pressure (kPa); (e_s-e_a) is vapor pressure deficit (Δe, kPa) at temperature T; T is daily mean air temperature (°C); ρ_a is mean air density at constant pressure (kg m^{-3}); c_p is specific heat of the air (MJ $kg^{-1}{}^{\circ}C^{-1}$); r_s is (bulk) surface resistance (s m^{-1}); and r_a is aerodynamic resistance (s m^{-1}), which is closely related to wind speed and surface characteristics.

Allen et al., 1998 standardized the PM equation as the FAO-PM model, assuming a hypothetical reference crop (short grass) with an assumed crop height of 0.12 m, a fixed surface resistance of 70 s m^{-1} and an albedo of 0.23, as

$$ET_0 = \frac{0.408\Delta(R_n - G) + \gamma(900/(T + 273))u_2(e_s - e_a)}{\Delta + \gamma(1 + 0.34u_2)} \quad (2)$$

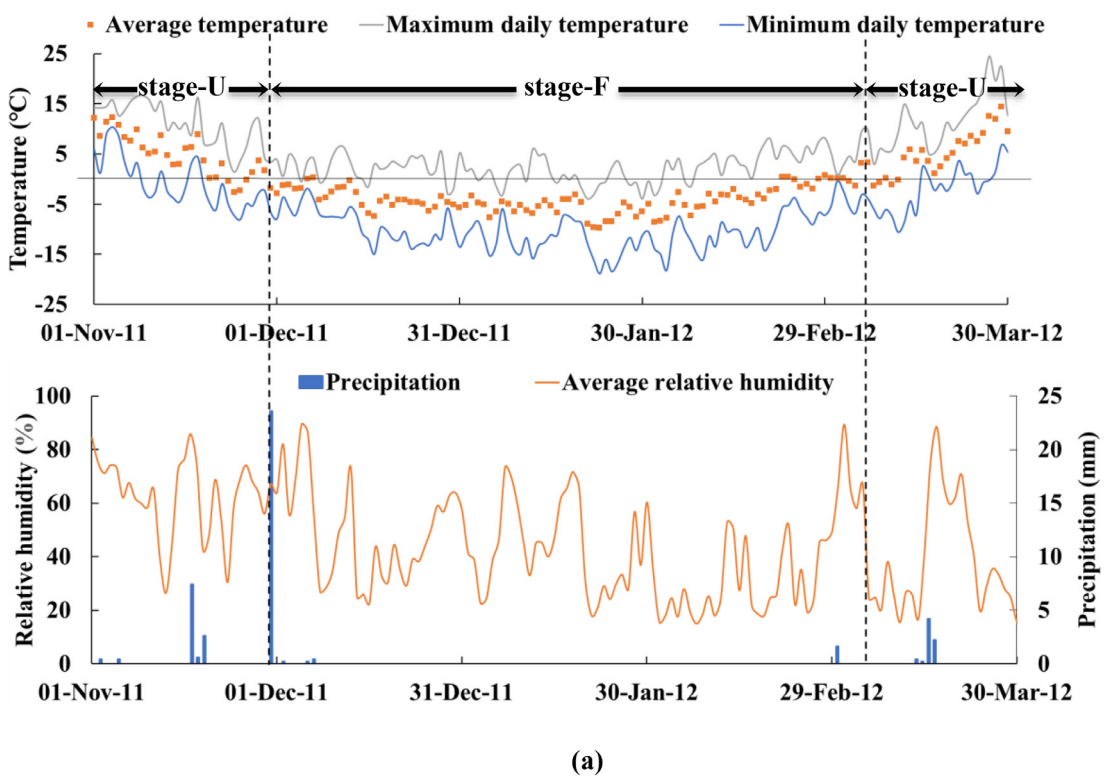

(a)

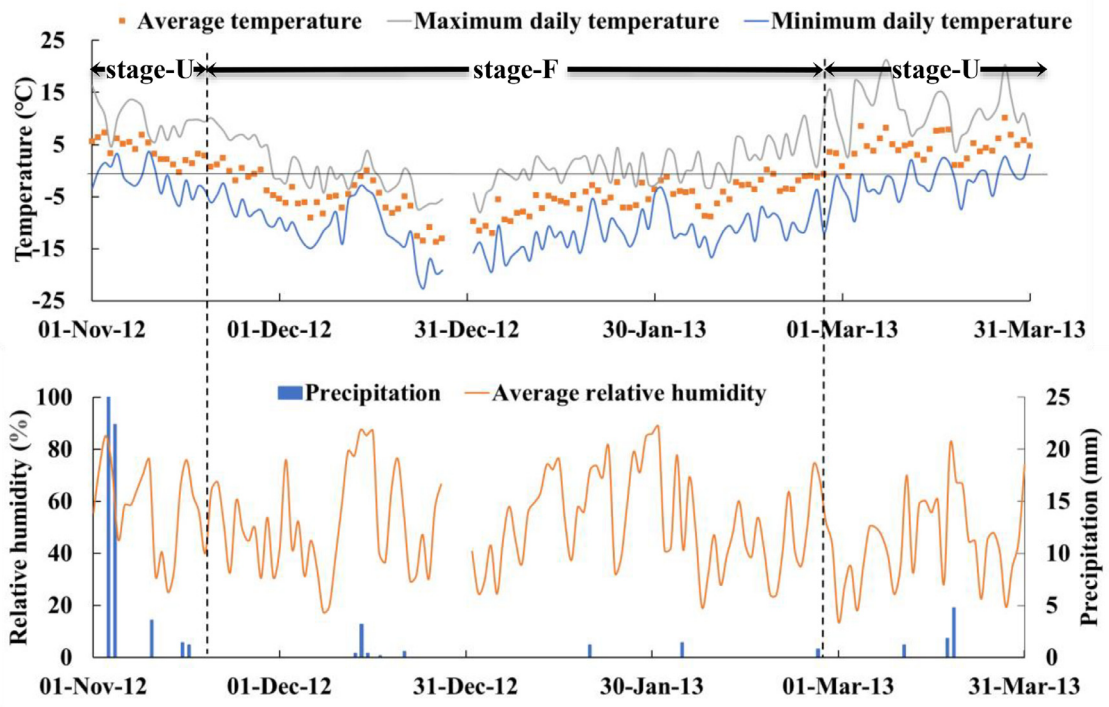

(b)

Fig. 2. Meteorological data over two winters: (a) 2011–2012, year 1; (b) 2012–2013, year 2.

where ET_0 is the reference ET (mm day^{-1}); u_2 is the average daily wind speed at 2 m height (m s^{-1}). When soil moisture is sufficient, ET is affected by meteorological factors adjusted for crop characteristics by a crop-specific coefficient (K_c) (Allen et al., 1998; Kang et al., 2003) as

$$ET_{PM} = K_c ET_0 \quad (3)$$

where ET_{PM} is the predicted ET using the FAO-PM model (mm day^{-1}). An average Kc of 0.4 was recommended by FAO for winter wheat during winter time (Allen et al., 1998).

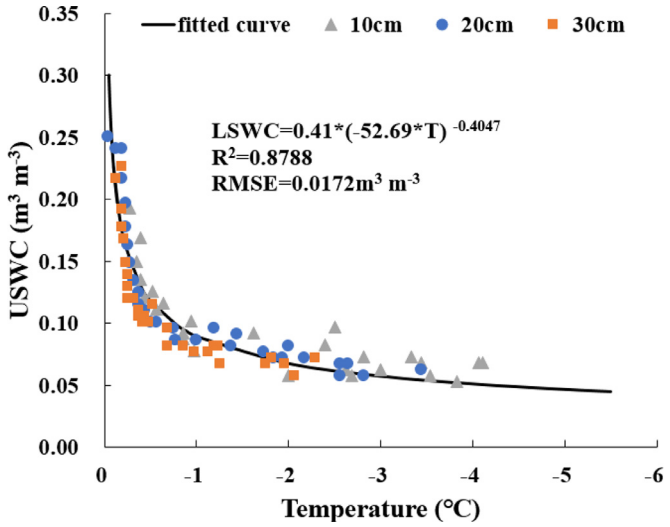

Fig. 3. Fitted soil freezing characteristics for optimizing soil hydraulic parameters using data obtained in year 1.

Table 2
Soil hydraulic parameters fitted for year 1.

Parameters	ψ_e (Pa)	b
Values	−850	2.5

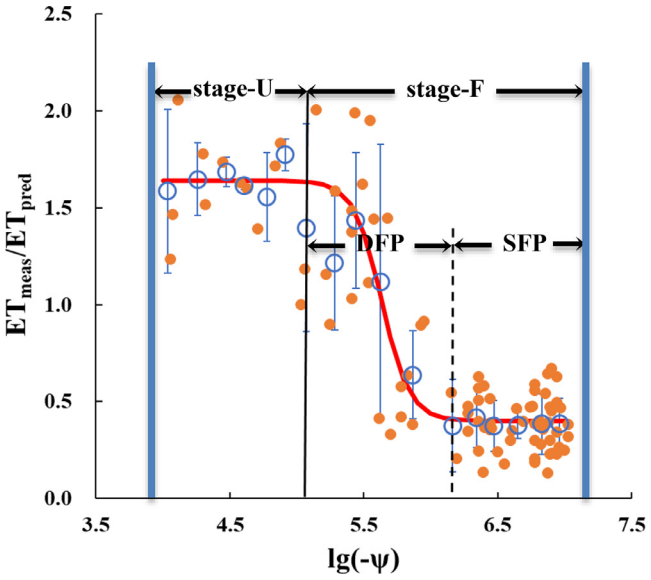

Fig. 5. Relationship ($R^2 = 0.819$) between the ratio of measured ET to predicted ET using Eq. (3) (ET_{meas}/ET_{pred}), and SWP at 10 cm depth in both stages in year 1. The frozen stage (stage-F) was separated into a stable frozen phase (SFP) and a dynamic frozen phase (DFP). The circles and error bars represent the average and standard deviation of ET_{meas}/ET_{pred}.

2.2. Experimental sites and procedures

The experiments were conducted at an experimental farm in Changping County, 35 km north of Beijing city center, China (116°26′39″ E, 40°10′43″ N). Average precipitation is 587 mm yr^{-1} and annual average temperature is 11.7°C at this location, with the freezing period generally from November to March.

The unfrozen soil water content (USWC) and soil temperature (T_{soil}) were obtained using a dielectric tube sensor (Cheng et al., 2014a; Spaans and Baker, 1996), and a digital temperature sensor (DS18B20, accuracy: 0.5 °C between −55 and 125 °C, Dallas Semiconductor, USA) over two winters (year 1: 2011–2012; year 2: 2012–2013). Lysimeters (24 independent units; 1 m in length, 0.75 m in width, 2.3 m in depth; Fig. 1a), filled with a sandy loam soil, were used to measure ET directly. Table 1 lists the soil textural and hydraulic properties. Winter wheat was planted in each lysimeter and all lysimeters were treated the same. Actual ET was predicted by weight difference at 15 min intervals with a sensitivity of 0.05–0.1 mm. The lysimeter facility is equipped with a weather station for obtaining on-site observations of solar radiation, air temperature, relative humidity, wind speed, and precipitation (Fig. 1b). Moreover, in the center of each lysimeter, one PVC access tube (1.4 m) was installed, vertically. The dielectric sensors were placed in the access tubes at 10 cm intervals. The temperature sensors were placed in a hole adjacent to each access tube at 10 cm intervals and backfilled with native soil. Three replicate soil samples were obtained at 10 cm and 20 cm in the field, respectively to determine saturated hydraulic conductivity (K_s) which was measured under laboratory conditions using the constant-head method (Klute, 1965).

2.3. Determination of soil freezing characteristic curve and soil hydraulic parameters

Simultaneous measurements of USWC and T_{soil} described a curve of soil freezing characteristic (SFC). Due to the similarity between soil moisture characteristic (SMC) curve and SFC curve (Spaans and Baker, 1996), SWP in unfrozen soil can be determined by measured

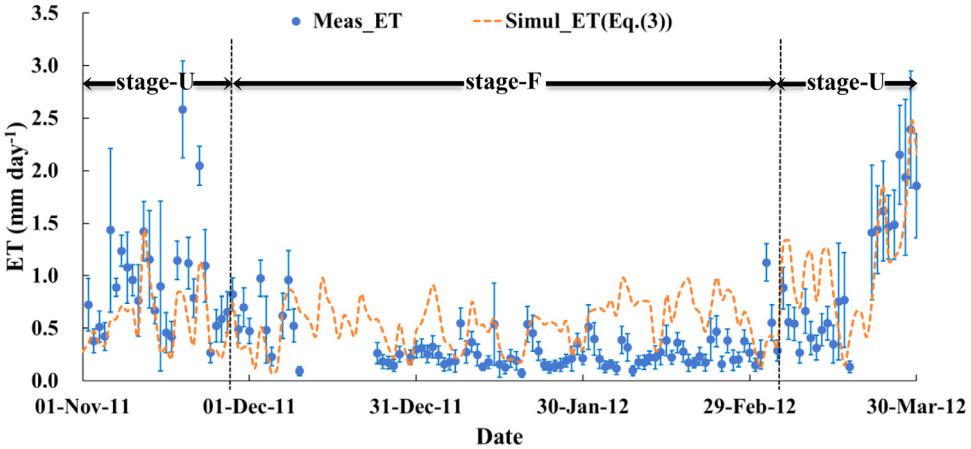

Fig. 4. Comparison between the measured ET and the predicted ET using Eq. (3) over the winter of year 1; the error bars are the standard deviation of measured ET with 24 lysimeters.

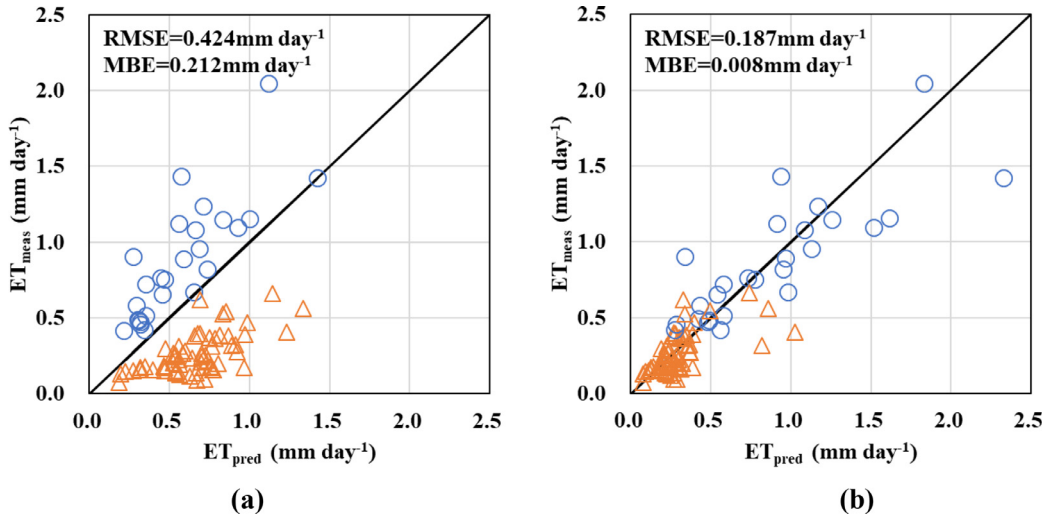

Fig. 6. Relationships between measured ET and predicted ET using (a) Eq. (3) or (b) Eq. (8) in the winter of year 1. The open circles represent the ET in stage-U while the open triangle points represent ET in stage-F.

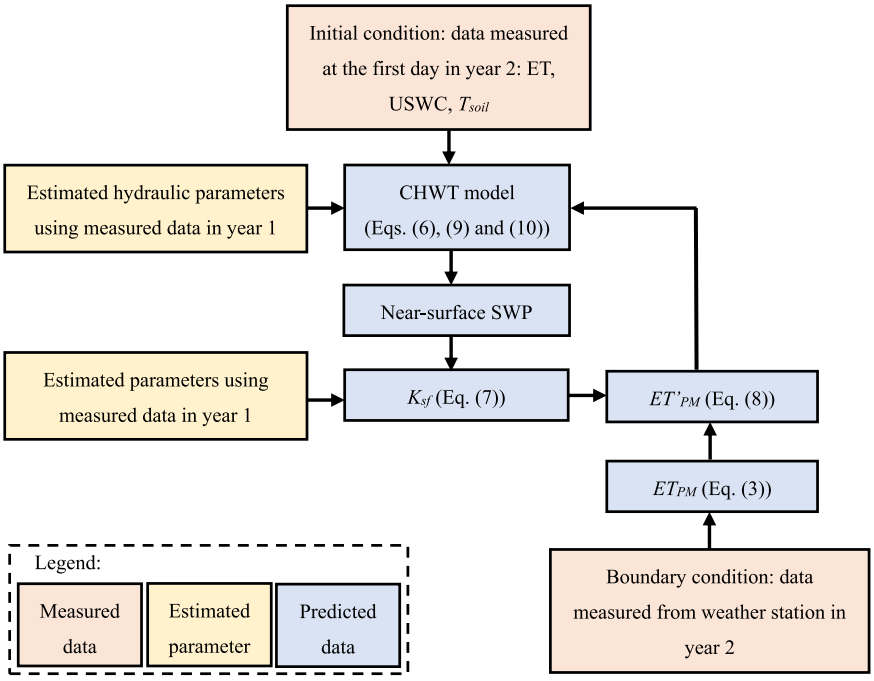

Fig. 7. The simulation procedure for the combined (FAOPM-K_{sf}-CHWT) model.

USWC and SMC curve derived from the SFC curve and the Clapeyron equation in frozen soil (Cheng et al., 2014a). The Campbell equation for describing SMC is expressed as

$$\psi = \psi_e \left(\frac{\theta_l}{\theta_s}\right)^{-b} \tag{4}$$

where ψ is the soil water potential (Pa); ψ_e is the air-entry potential (Pa); b is a pore size distribution parameter, θ_l is the USWC ($m^3\ m^{-3}$); and θ_s is the saturated soil water content ($m^3\ m^{-3}$).

The Clapeyron equation in frozen soil is expressed as

$$\psi = \frac{L_f}{g}\frac{T_{soil}}{T_k} \quad T_{soil} < 0 \tag{5}$$

where T_k absolute temperature (K); L_f is the latent heat of fusion (334 kJ kg^{-1}); g is the acceleration due to gravity (m s^{-2}).

The SFC was determined within the soil profile for year 1 by inversion of the Campbell (Eq. (4)) and the Clapeyron (Eq. (5)) equations (Cheng et al., 2014a, 2019) and expressed as:

$$\theta_l = \theta_s \left(\frac{L_f}{g\psi_e}\frac{T_{soil}}{T_k}\right)^{-\frac{1}{b}} T_{soil} < 0 \tag{6}$$

Fitting Eq. (6) with direct measurements allowed values of ψ_e and b to be optimized. Then the SWP in unfrozen soil can be estimated using Eq. (4).

3. Results and discussion

3.1. Meteorological data

The average daily temperature (T_{ave}) in year 1 was below zero from Nov. 30, 2011 to Mar. 5, 2012 (Fig. 2a) and in year 2 from Nov. 23, 2012 to Feb. 26, 2013 (Fig. 2b). Precipitation was higher in the winter

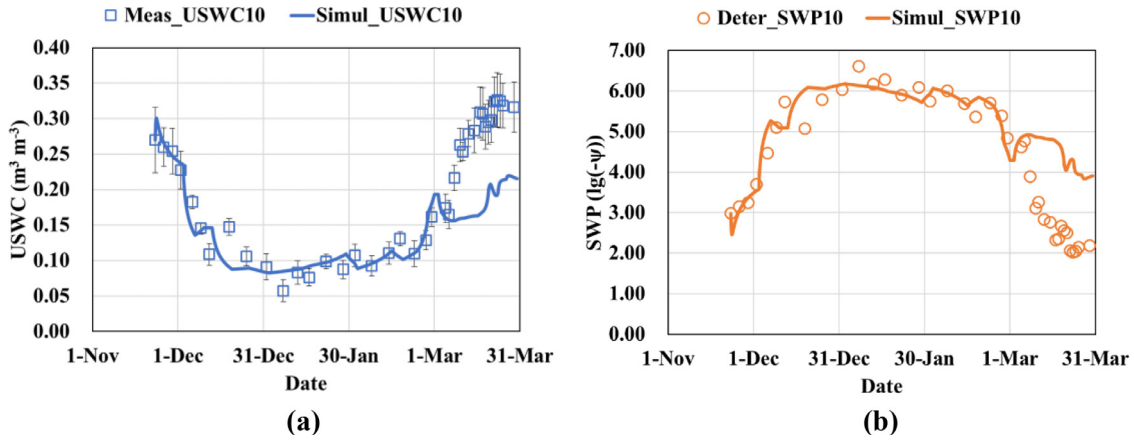

Fig. 8. Comparison in year 2 between the measured and the simulated (a) USWC and (b) SWP at 10 cm (measured or determined data, open symbols; simulated data, solid line).

of year 2 than that in the winter of year 1 (cf. Fig. 2a and b).

Based on T_{ave}, the winter season in both years can be separated into two stages, one characterized by unfrozen soil with $T_{ave} > 0$ (stage-U) and the other with mostly frozen soil with $T_{ave} \leq 0$ (stage-F). The environmental parameters, air temperature, relative humidity, precipitation, wind speed and net radiation measured in year 1, were used to predict ET in year 1, using Eq. (3) (the FAO-PM model with $K_c = 0.4$).

3.2. Results of determined SFC curve and soil hydraulic parameters

By fitting Eq. (6) with direct measurements (Figure 3), ψ_e and b were optimized, as shown in Table 2. These optimized soil hydraulic parameters (from year 1) were used to predict SWP (Eq. (4)) in the winter of year 2.

3.3. Correction of ET prediction by a freezing coefficient

3.3.1. Comparison between measured and predicted ET using the FAO-PM model

Figure 4 shows the time courses of measured ET and predicted ET, calculated using Eq. (3) with $K_c = 0.4$ over the winter of year 1. Eq. (3) underestimated ET in stage-U and overestimated ET in stage-F. The ratio of measured ET to predicted ET was strongly dependent on SWP at 10 cm in a sigmoidal fashion (Fig. 5).

Stage-F presents in two phases: a stable frozen phase (SFP) and a transitional dynamic frozen phase (DFP). In stage-F/SFP and stage-U, the ratio is almost independent of SWP, with strikingly different ratios of ET_{meas}/ET_{pred} (0.4 and 1.64, respectively). The phase change of liquid water to ice, or the reverse, altered the available soil water and the migration paths of both liquid and vapor phase water in the soil.

3.3.2. Improvement of ET prediction by correction for soil freezing

ET_{meas}/ET_{pred} was strongly related to SWP. To incorporate this relationship into the FAO-PM framework, we propose this ratio as a freezing stress index, $K_{sf} = ET_{meas}/ET_{pred}$, as a function of SWP to improve the prediction of ET in winter. We relate K_{sf} to SWP estimated in year 1 using a sigmoidal regression (Fig. 5), as

$$K_{sf} = \frac{1.24}{1 + e^{9.483*(\lg(-\psi)-5.634)}} + 0.4 \tag{7}$$

and modify Eq. (3) as

$$ET'_{PM} = K_c K_{sf} ET_0 \tag{8}$$

The poor agreement (RMSE = 0.424 mm day^{-1}; Fig. 6a) of modeled and measured ET calculated using Eq. (3) in year 1 is substantially improved using the modification in Eq. (8); RMSE = 0.187 mm day^{-1}; Fig. 6b). This demonstrated the concept, using the same data to parameterize the modified model, that ET prediction can be improved by considering variations of SWP over the entire winter. We then tested this approach using the independent data set obtained in year 2.

3.4. Combination of the freezing-corrected FAO-PM model with a coupled heat and water transfer (CHWT) model

During soil freezing-thawing cycles, the phase change between water and ice alters USWC and thus available near-surface SWC, and consequently changes the paths of unfrozen liquid and vapor water movement. Associated energy exchange further affects the temperature distribution. CHWT models have been widely used to relate T_{soil}, SWP and USWC in frozen soil (Harlan, 1973; Flerchinger and Saxton, 1989; Jame and Norum et al., 1980; Zhao et al., 1997; Šimůnek et al., 1998). We combine a CHWT model with Eq. (8); following Cheng et al. (2014b) as

$$\frac{\partial \theta_l}{\partial t} + \frac{\rho_i}{\rho_l}\frac{\partial \theta_i}{\partial t} = \frac{\partial}{\partial t}\left[D(\theta_l)\frac{\partial \theta_l}{\partial z} - K(\theta_l)\right] + U \tag{9}$$

$$C_s\frac{\partial T_{soil}}{\partial t} - \rho_i L_f \frac{\partial \theta_i}{\partial t} + L_v\left(\frac{\partial q_v}{\partial z} - \frac{\partial \rho_v}{\partial t}\right) = \frac{\partial}{\partial z}\left(\lambda_s \frac{\partial T_{soil}}{\partial z}\right) + \rho_l c_l \frac{\partial q_l T_{soil}}{\partial z} + S \tag{10}$$

where θ_i represents ice soil water content (m^3 m^{-3}); ρ_l, ρ_i and ρ_v denote the densities of unfrozen water, ice and vapor (kg m^{-3}), respectively; K is unsaturated hydraulic conductivity (m h^{-1}); D is the water diffusivity (m^2 h^{-1}); C_s is volumetric heat capacity (J kg^{-1} °C^{-1}) of the soil; q_l and q_v are the liquid water vapor flux (kg s^{-1} m^{-2}); λ_s is soil thermal conductivity (W m^{-1} °C^{-1}); c_l is specific heat capacity of water (J kg^{-1} °C^{-1}); L_v is the latent heat of evaporation (kJ kg^{-1}); z is vertical distance within soil profile (m); U is a source/sink term for water flux associated with root water uptake and S represents the uptake of energy associated with root water uptake (m^3 m^{-3} s^{-1}). The optimized soil hydraulic parameters in Table 2 were used as the initial conditions of the CHWT model.

The simulation procedure for the combined (FAOPM-K_{sf}-CHWT) model in detail in year 2 is described in Fig. 7. The boundary conditions using the meteorological data and the initial conditions of T_{soil}, USWC and ET were measured in the field in year 2. The soil hydraulic parameters in the CHWT model and the parameters in K_{sf} (Eq. (7)) were estimated from the measurements in year 1. The USWC, SWP, K_{sf} and ET in year 2 were predicted by numerical simulation using the combined model.

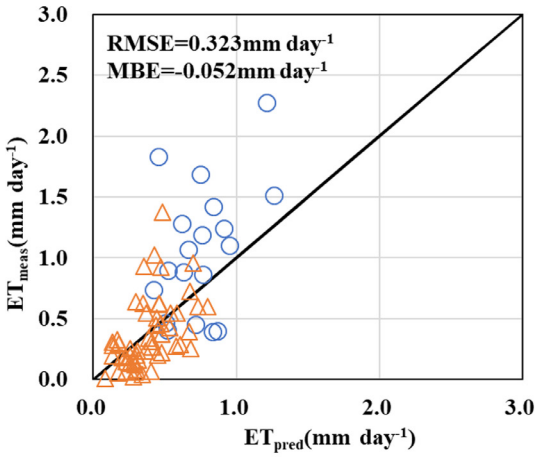

(a)

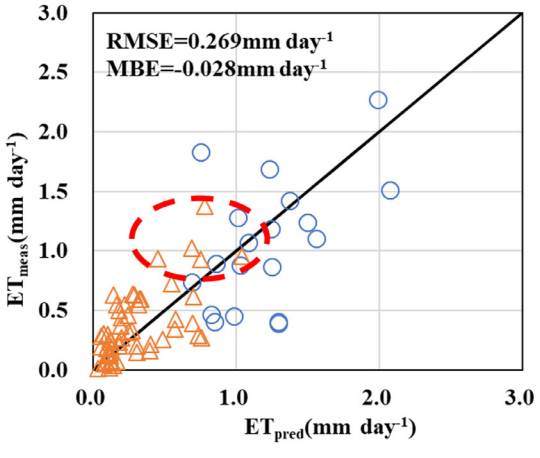

(b)

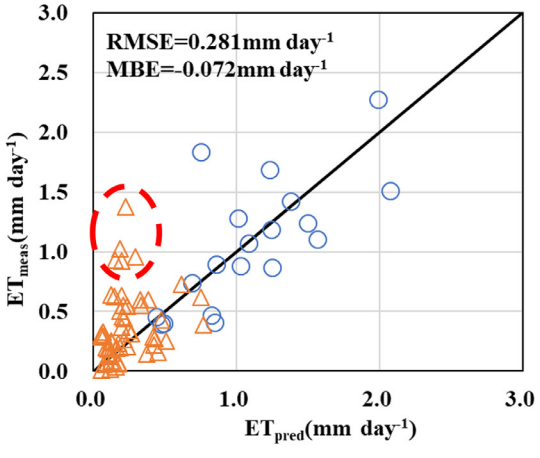

(c)

Fig. 9. Comparison in year 2 between the measured ET and the predicted ET using (a) the FAO PM model (Eq. (3)), (b) the combined model with the determined SWP or (c) the combined model with the simulated SWP. The open circles represent the ET in stage-U while the open triangle points represent ET in stage-F. The values of open triangle points in red dotted circle in Fig. 9c represent the underestimation of predicted ET in comparison with those values in Fig. 9b due to the underestimation of USWC and SWP (Fig. 8, Dec. 17, 2012 to Dec. 23, 2012) in year 2.

3.5. *Test of the combined FAOPM-K_{sf}-CHWT model in year 2*

3.5.1. *Comparison between simulated and measured/determined USWC and SWP*

USWC and SWP (at 10 cm) simulated by the combined model were shown in Fig. 8. The numerical simulation of USWC and SWP generally agreed well with measured or determined values in year 2 (Fig. 8). These predictions of SWP allowed determination of the corresponding K_{sf} using Eq. (7).

3.5.2. *Comparison between predicted and measured ET using the combined model in year 2*

Predicted ET was compared with measurements of ET in year 2 to exercise the combined model using independent data. ET predicted using Eq. (3) (Fig. 9a) consistently underestimated measured ET in stage-U and overestimated in stage-F, in year 2 as observed in year 1 (cf. Fig. 6a). Incorporation of SWP at 10 cm, whether determined (Fig. 9b) or simulated (Fig. 9c), and incorporation of the appropriately re-calculated K_{sf} improved the prediction accuracy relative to Eq. (3). RMSE of the model predictions improved from 0.323 mm day^{-1} to 0.269 mm day^{-1} using determined data and to 0.281 mm day^{-1} using simulated data (Fig. 9a, b, c, respectively). In Fig. 8b, simulated SWP from the CHWT model was somewhat less accurate than that using the determined SWP (Eq. (4)) from SFC (Eq. (6)) and the Clapeyron equation (Eq. (5)). This may contribute to the underestimation of USWC and SWP (Dec. 17, 2012 to Dec. 23, 2012), and the resulting underestimation of K_{sf} and predicted ET (the values of open triangle points in red dotted circle in Fig. 9c).

Because ET is controlled by SWP, the current correction based on SWP rather than SWC provides a more universal approach which overcomes limitations due to site-specific soil conditions. As SWP in frozen soil is strongly correlated with T_{soil} (the Clapeyron equation), remote sensing of land surface temperature may prove useful in determining K_{sf} at larger scale. This and further elaborations have great potential to render the incorporation of K_{sf} into the combined model as a key step in improving estimation of ET in winter.

4. Conclusions

We have identified inadequacies in the standard FAO-PM model of ET during wintertime. We address these deficiencies by separating winter conditions into stable frozen and unfrozen stages, separated by a transitional dynamic phase. The standard model under-predicts ET in stage-U (unfrozen soil) and over-predicts ET in stage-F (frozen soil). We suggest a new freeze stress index, K_{sf}, defined as a function of SWP at 0–10 cm. A CHWT model was introduced to estimate SWP. Incorporation of K_{sf} and CHWT into a combined model improved the RMSE of ET predictions from 0.323 mm day^{-1} to 0.281 mm day^{-1} in year 2, using the meteorological data of year 2 as boundary conditions, and initial values of year 2 and soil properties determined in year 1 as initial conditions. The combined model reduces the requirement for data from frozen soil and extends the application of the FAO-PM model to non-cropping seasons including winter in temperate climates. Future work is suggested to introduce remote sensing techniques into the proposed combined (FAOPM-K_{sf}-CHWT) model to determine ET at larger scales during winter.

Declaration of Competing Interest

The authors declare that they have no known competing financial interests or personal relationships that could have appeared to influence the work reported in this paper.

Acknowledgments

We acknowledge financial supports from the National Natural

Science Foundation of China under project no. 31871527 and project no. 31971576. We also acknowledge financial supports of the Chinese-German Center for Scientific Promotion(Chinesisches-Deutsches Zentrum fuer Wissenschaftsfoerderung) under project no. GZ1272.

References

Adeloye, A.J., Rustum, R., Kariyama, I.D., 2012. Neural computing modeling of the reference crop evapotranspiration. Environ. Modell. Softw. 29 (1), 61–73.

Ali, M., Hamideh, N., Majid, V., Mahdi, B., 2018. Estimating net irrigation requirement of winter wheat using model- and satellite-based single and basal crop coefficients. Agric. Water Manag. 208, 95–106.

Allen, R.G., Pereira, L.S., Raes, D., Smith, M., 1998. Crop evapotranspiration-Guidelines for computing crop water requirements-FAO Irrigation and drainage paper 56 300(9). FAO, Rome, pp. D05109.

Bodner, G., Loiskandl, W., Kaul, H.P., 2007. Cover crop evapotranspiration under semi-arid conditions using fao dual crop coefficient method with water stress compensation. Agricul. Water Manag. 93 (3) 0-98.

Cai, J., Liu, Y., Lei, T., Pereira, L.S., 2007. Estimating reference evapotranspiration with the fao penman–monteith equation using daily weather forecast messages. Agri. For. Meteorol. 145 (1–2) 0-35.

Chanzy, A., Bruckler, L., 1993. Significance of soil surface moisture with respect to daily bare soil evaporation. Water Resour. Res. 29 (4).

Cheng, Q., Sun, Y., Xue, X., Guo, J., 2014a. In situ determination of soil freezing characteristics for estimation of soil moisture characteristics using a dielectric tube sensor. Soil Sci. Soc. Am. J. 78 (78), 133–138.

Cheng, Q., Sun, Y., Jones, S.B., Vasilyev, V.I., Popov, V.V., Wang, G., Zheng, L., 2014b. In situ measured and simulated seasonal freeze–thaw cycle: a 2-year comparative study between layered and homogeneous field soil profiles. J. Hydrol. 519, 1466–1473.

Cheng, Qiang, Xu, Q., Cheng, X., Yu, S., Wang, Z., Sun, Y., Yan, X., Jones, S.B., 2019. In-situ estimation of unsaturated hydraulic conductivity in freezing soil using improved field data and inverse numerical modeling. Agri. For. Meteorol. 279, 107746.

Ding, R., Kang, S., Li, F., Zhang, Y., Tong, L., 2013. Evapotranspiration measurement and estimation using modified Priestley–Taylor model in an irrigated maize field with mulching. Agri. For. Meteorol. 168 (1), 140–148.

Flerchinger, G.N., Saxton, K.E., 1989. Simultaneous heat and water model of a freezing snow-residue-soil system I. Theory and development [J]. Trans. Am. Soc. Agri. Eng. 32 (2), 565–571.

Harlan, R.L., 1973. Analysis of coupled heat-fluid transport in partially frozen soil. Water Resour. Res. 9 (5), 1314–1323.

Huo, Z., Feng, S., Kang, S., Dai, X., 2012. Artificial neural network models for reference evapotranspiration in an arid area of northwest china. J. Arid Environ. 82, 0–90.

Hssaine, B.A., Merlin, O., Rafi, Z., Ezzahar, J., Jarlan, L., Khabba, S., Er-Raki, S., 2018. Calibrating an evapotranspiration model using radiometric surface temperature, vegetation cover fraction and near-surface soil moisture data. Agri. For. Meteorol. 256-257, 104–115.

Jame, Y.W., Norum, D.I., 1980. Heat and mass transfer in a freezing unsaturated porous medium. Water Resour. Res. 16 (4), 811–819.

Jiang, X., Kang, S., Li, F., Du, T., Tong, L., Comas, L., 2016. Evapotranspiration partitioning and variation of sap flow in female and male parents of maize for hybrid seed production in arid region. Agric. Water Manag. 176, 132–141.

Kang, S., Gu, B., Du, T., Zhang, J., 2003. Crop coefficient and ratio of transpiration to evapotranspiration of winter wheat and maize in semi-humid region. Agric. Water Manag. 59 (3), 239–254.

Klute, A., 1965. Laboratory measurement of hydraulic conductivity of saturated soil. Methods of soil analysis. Agron. Monogr.

Liu, S., Graham, W.D., Jacobs, J.M., 2005. Daily potential evapotranspiration and diurnal climate forcings: influence on the numerical modelling of soil water dynamics and evapotranspiration. J. Hydrol. (Amsterdam) 309 (1–4), 0–52.

Liu, X., Xu, C., Zhong, X., Li, Y., Yuan, X., Cao, J., 2017. Comparison of 16 models for reference crop evapotranspiration against weighing lysimeter measurement. Agric. Water Manag. 184, 145–155.

Monteith, J.L., 1965. Evaporation and environment. Symp. Soc. Exp. Biol. 19 (19), 205–234.

Merlin, O., Olivera-Guerra, L., AiT Hssaine, B., Amazirh, A., Rafi, Z., Ezzahar, J., Gentine, P., Khabba, S., Gascoin, S., Er-Raki, S., 2018. A phenomenological model of soil evaporative efficiency using surface soil moisture and temperature data. Agri. For. Meteorol. 256-257, 501–515.

Mitchell, P.J., Veneklaas, E., Lambers, H., Burgess, S.S.O., 2009. Partitioning of evapotranspiration in a semi-arid eucalypt woodland in south-western Australia. Agri. For. Meteorol. 149 (1), 0–37.

Haymann, N., Lukyanov, V., Tanny, J., 2019. Effects of variable fetch and footprint on surface renewal measurements of sensible and latent heat fluxes in cotton. Agri. For. Meteorol. 268, 63–73.

Penman, H.L., 1948. Natural evaporation from open water, bare soil and grass. Proc. Roy. Soc. London, Ser. A: Math. Phys. Sci. 193 (1032), 120–145.

Phogat, V., Šimůnek, J., Skewes, M.A., Cox, J.W., Mccarthy, M.G., 2016. Improving the estimation of evaporation by the fao-56 dual crop coefficient approach under subsurface drip irrigation. Agric. Water Manage. 178, 189–200.

Poulovassilis, A., Anadranistakis, M., Liakatas, A., Alexandris, S., Kerkides, P., 2001. Semi-empirical approach for estimating actual evapotranspiration in greece. Agricul. Water Manag. 51 (2), 0–152.

Rana, G., Katerji, N., 2000. Measurement and estimation of actual evapotranspiration in the field under Mediterranean climate: a review. Eur. J. Agron. 13 (2–3), 125–153.

Raz-Yaseef, N., Rotenberg, E., Yakir, D., 2010. Effects of spatial variations in soil evaporation caused by tree shading on water flux partitioning in a semi-arid pine forest. Agric. For. Meteorol. 150, 454–462.

Sentelhas, P.C., Gillespie, T.J., Santos, E.A., 2010. Evaluation of FAO Penman–Monteith and alternative methods for estimating reference evapotranspiration with missing data in southern Ontario, Canada. Agric. Water Manag. 97 (5) 0-644.

Šimůnek, J., Van Genuchten, M.T., Wendroth, O., 1998. Parameter estimation analysis of the evaporation method for determining soil hydraulic properties. Soil Sci. Soc. Am. J. 62 (4), 894.

Snyder, R.L., Bali, K., Ventura, F., Gomez-Macpherson, H., 2000. Estimating evaporation from bare or nearly bare soil. J. Irrigation. Drain. Eng. 126 (6), 399–403.

Spaans, E.J.A., Baker, J.M., 1996. The soil freezing characteristic: its measurement and similarity to the soil moisture characteristic. Soil Sci. Soc. Am. J. 60, 13–19.

Tomas-Burguera, M., Vicente-Serrano, S.M., Grimalt, M., Beguería, S., 2017. Accuracy of reference evapotranspiration (ET0) estimates under data scarcity scenarios in the iberian peninsula. Agric. Water Manage. 182, 103–116.

Torres, A.F., Walker, W.R., Mckee, M., 2011. Forecasting daily potential evapotranspiration using machine learning and limited climatic data. Agric. Water Manage. 98 (4) 0-562.

Zhang, Y., Kang, S., Ward, E.J., Ding, R., Zhang, X., Zheng, R., 2011. Evapotranspiration components determined by sap flow and microlysimetry techniques of a vineyard in northwest china: dynamics and influential factors. Agric. Water Manage. 98 (8) 0-1214.

Zhang, Z., Wang, W., Gong, C., Wang, Z., Yu, P., 2019. Evaporation from seasonally frozen bare and vegetated ground at various groundwater table depths in the ordos basin, northwest China. Hydrol. Processes.

Zhao, L., Gray, D.M., Male, D.H., 1997. Numerical analysis of simultaneous heat and mass transfer during infiltration into frozen ground. J. Hydrol. 200 (1–4), 345–363.

Zhao, P., Kang, S., Li, S., Ding, R., Tong, L., Du, T., 2018. Seasonal variations in vineyard et partitioning and dual crop coefficients correlate with canopy development and surface soil moisture. Agric. Water Manage. 197, 19–33.